Generation of excess Si species at Si/SiO$_2$ interface and their diffusion into SiO$_2$ during Si thermal oxidation

Kenzo Ibano, Kohei M. Itoh, and Masashi Uematsu[a)]

Department of Applied Physics and Physico-Informatics, Keio University, Yokohama 223-8522, Japan

Si self-diffusion in thermally grown SiO$_2$ near the SiO$_2$/Si interface during thermal oxidation process was studied using isotopic heterostrucutures (^{nat}SiO$_2$/^{28}Si) as a function of the oxidation temperature, the oxidation time, and the fraction of oxygen in the ambient gas. The Si self-diffusivity near the SiO$_2$/Si interface during oxidation was found to be larger than the thermal Si self-diffusivity by more than one order of magnitude. This enhancement indicates that Si species are emitted from the SiO$_2$/Si interface and diffused into SiO$_2$ during oxidation, as has been predicted by recent theoretical studies. © *2008 American Institute of Physics*.
[DOI: 10.1063/1.2831293]

The fundamental understanding of the atomic phenomena during the processing of a semiconductor integrated circuit, especially the formation mechanism of ultrathin silicon dioxide (SiO$_2$), is highly important for the electronic industry. The high-temperature thermal treatment of Si substrates in O$_2$ ambient causes a reaction to grow SiO$_2$ layers at the SiO$_2$/Si interface. While the oxidation rate for the thick (>30 nm) oxide films is explained by the oxygen diffusion through SiO$_2$ layer or by the reaction of Si and O$_2$ at the SiO$_2$/Si interface, the fast oxidation rate for the thinner oxide films cannot be predicted by Deal-Grove model,[1] and this fast oxidation rate is known as initial oxidation enhancement. As an explanation for the faster growth mechanism, the Si emission model has been proposed, where Si species are emitted from the interface during oxidation to release the oxidation-induced stress, and this emission governs the oxidation rate.[2–4] There have been a number of suggestions, based on theoretical and experimental studies, regarding emission of Si species from the interface to SiO$_2$.[4–8] In addition, the Si emission to SiO$_2$ is consistent with the formation of oxidation-induced stacking faults in the Si substrates.[9]

Although a number of experimental studies[10,11] have been performed to directly observe the emitted Si species during oxidation, no concrete evidence has been reported. Therefore, the purpose of this study is to observe the Si species emitted from the interface and diffused into SiO$_2$ during oxidation by investigating the Si self-diffusion in SiO$_2$. While a recent study observed the accumulation of Si at the surface of the HfO$_2$/SiO$_2$/Si structure,[8] the present report shows the enhanced Si self-diffusion near the SiO$_2$/Si interface, which is a direct evidence of Si emission to SiO$_2$ during the oxidation. In addition, the Si self-diffusivity enhanced by the emitted Si was obtained.

In the previous report,[12] the Si self-diffusion in SiO$_2$ was investigated by the diffusion profiles of implanted ^{30}Si in ^{28}SiO$_2$. In this experiment, no enhancement of Si self-diffusivity was observed during oxidation. We assumed that

the distance between the SiO$_2$/Si interface and ^{30}Si diffusers was too large to observe the enhancement during oxidation because the emitted Si species are oxidized near the SiO$_2$/Si interface by oxygen diffusing from the surface before the Si species reach the region where ^{30}Si diffusion is taking place. In the present study, we used the samples with the structure of ^{nat}SiO$_2$/^{28}Si [Fig. 1(a)] so that the distance between ^{30}Si in ^{nat}SiO$_2$ and the SiO$_2$/Si interface is minimal. With this approach, we observed the enhanced Si self-diffusion near the Si/SiO$_2$ interface during oxidation.

The samples used in the present work were prepared as follows. An isotopically enriched ^{28}Si epilayer of 800 nm thickness grown by chemical vapor deposition (CVD) was provided by Isonics Corp., Colorado, USA. The isotope compositions measured with secondary ion mass spectrometry (SIMS) were ^{28}Si(99.924%), ^{29}Si(0.073%), and ^{30}Si(0.003%). The sample was completed by deposition of ^{nat}SiO$_2$ with thickness of 22 nm on the surface of ^{28}Si by low-pressure CVD using tetraethoxysilan at 700 °C and the structure is shown in Fig. 1(a). All samples were cut into 5 ×5 mm^2 pieces and oxidized in a resistance furnace at temperatures of 1150, 1200, and 1250 °C in time periods between 30 min and 16 h. Semiconductor processing grade quartz tube and gas source were employed to keep the sample as clean as possible. The samples were oxidized under flowing argon with 1%, 10%, and 100% oxygen fractions in order to investigate the influence of the oxidation rate. In this oxidation, ^{28}SiO$_2$ layer was grown, as shown in Fig. 1(b). Then, the ^{30}Si self-diffusion from the ^{nat}SiO$_2$ layer into
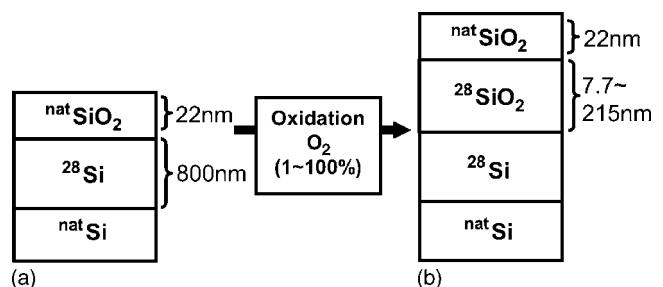

FIG. 1. Schematic of silicon dioxide isotope heterostructures.

---

a)Also at NTT Basic Research Laboratories until February 2007. Electronic mail: uematsu@a3.keio.jp.
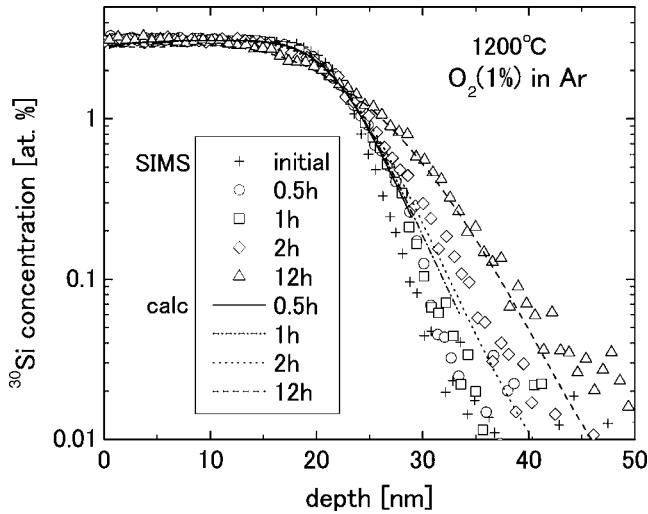
103, 026101-1

FIG. 2. SIMS (symbols) and calculated (lines) profiles of ^{30}Si in the isotope heterostructures before and after oxidation with the oxygen fraction of 1% in argon ambient at 1200 °C for 0.5, 1, 2, and 12 h, where the total SiO$_2$ thicknesses are 31, 34, 43, and 83 nm, respectively. The calculated profiles in the SiO$_2$ regions are shown.

FIG. 3. The grown ^{28}SiO$_2$ thickness dependence of Si self-diffusion coefficients in SiO$_2$: $\square$, $\bigcirc$, and $\triangle$ represent the results of oxidation at 1150 °C under 1%, 10%, and 100% oxygen in argon, respectively. The dashed line shows the thermal equilibrium Si self-diffusivity from Ref. 14, which is independent of the distance from the interface.

the newly grown ^{28}SiO$_2$ layer during oxidation was observed by SIMS. In the oxidation experiments, short oxidation times and low oxygen fractions were chosen to make the ^{28}SiO$_2$ layers thin so that the enhanced Si self-diffusion is clearly observed. Note that the diffusion length $(2\sqrt{Dt})$ of ^{30}Si did not surpass the thickness of the grown ^{28}SiO$_2$ layer in the present oxidation conditions. For example, in the 1 h oxidation at 1150 °C in the 1% oxygen fraction, which makes the thinnest ^{28}SiO$_2$ layer among the present study, the diffusion length and the thickness of the grown ^{28}SiO$_2$ layer were 3.7 and 7.7 nm, respectively.

Diffusion profiles of Si isotopes and oxygen of ^{nat}SiO$_2$/^{28}SiO$_2$/^{28}Si were measured by SIMS using O$_2^+$ ions as a primary ion beam with acceleration energy of 5 keV. An electron beam was irradiated on the sample during the SIMS measurement to prevent the sample from charge up. Each sample was measured at least twice to avoid the risk of measurement errors. In some samples, the change in the oxide thickness is so slight that the following method was used to minimize the errors in depth. The total oxide thickness of each sample after oxidation was measured by ellipsometry to determine the depth of the SiO$_2$/Si interface from the surface. In the SIMS profiles, the interface depth was determined from the position where the ^{16}O signal intensity falls to $1/e$ of its stationary value at the SiO$_2$/Si interface. The depth of SIMS profiles was determined so that the interface position is equal to the oxide thickness.

Figure 2 shows the depth profiles of ^{30}Si near the interface of ^{nat}SiO$_2$/^{28}SiO$_2$. As this figure shows, the ^{nat}SiO$_2$/^{28}Si interface of the initial (not oxidized) profile is broadened, although this initial profile should be a sharp step function whose concentration falls from 3.1% to 0.003% at the ^{nat}SiO$_2$/^{28}Si interface. This broadening is inherent in SIMS measurements and is caused by ion mixing due to ion sputtering. Because this ion mixing effect of SIMS measurement is different between the SiO$_2$ layer and the Si substrate, the characteristic parameters for the mixing, roughness, and in-
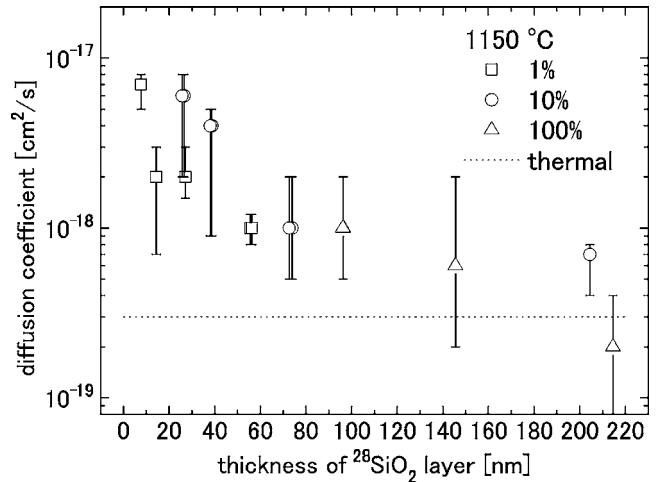
formation (MRI) analysis,[13] which are needed for the correction of the instrumental broadening, were determined from the profile of the sample that initially has the ^{nat}SiO$_2$(22 nm)/^{28}SiO$_2$ structure, which is different from the ^{nat}SiO$_2$/^{28}SiO$_2$/^{28}Si sample mentioned above. In order to obtain the MRI parameters, a convolution integral is applied to the sharp step profile to fit the SIMS profile of the ^{nat}SiO$_2$/^{28}SiO$_2$ sample. The depth profiles of ^{30}Si in the oxidized samples were modeled by

$$C(x) = C_{28} + \frac{C_{nat} - C_{28}}{2}\left[\mathrm{erf}\left(\frac{x+h}{2\sqrt{Dt}}\right) - \mathrm{erf}\left(\frac{x-h}{2\sqrt{Dt}}\right)\right], \quad (1)$$

which is a solution of Fick's second law for the isotopic heterostructure. In the equation, C_{nat} and C_{28} are the initial ^{30}Si concentrations in ^{nat}SiO$_2$ and ^{28}SiO$_2$, respectively, $x=0$ is the surface of samples, h is the depth of the ^{nat}SiO$_2$/^{28}SiO$_2$ interface, t is the annealing time, and D is the Si self-diffusion coefficient in SiO$_2$. In order to obtain the diffusion coefficients, Eq. (1) is applied to the sharp step profile to simulate the profiles after the oxidation in Fig. 2. Then, these diffusion profiles are broadened by the convolution integral mentioned above to reproduce the profiles in Fig. 2. We choose the appropriate value of D in Eq. (1) so that the diffused and broadened profiles are comparable to the SIMS profiles in Fig. 2, where the calculated profiles in the SiO$_2$ regions are shown. Even though the sample used in this study does not initially have the ^{nat}SiO$_2$/^{28}SiO$_2$ interface, we calculated as though because a few nanometer initial natural-grown ^{28}SiO$_2$ layers may exist, and in addition, the diffusion length did not surpass the thickness of the grown ^{28}SiO$_2$ layer.

Diffusion coefficients obtained in this study are shown in Figs. 3 and 4, both of which have x axis of the grown ^{28}SiO$_2$ thickness. Figure 3 clearly shows increasing self-diffusivity with decreasing thickness of the ^{28}SiO$_2$ layer. The diffusivity approaches the thermal equilibrium value[14] as the thickness of the ^{28}SiO$_2$ layer increases. This thermal equilibrium value was obtained from the ^{nat}SiO$_2$(50 nm)/^{28}SiO$_2$(650 nm)/^{28}Si
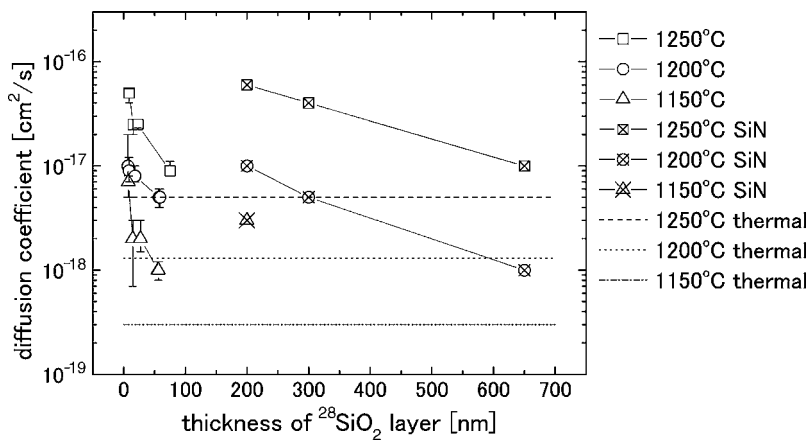
FIG. 4. The $^{28}SiO_2$ thickness dependence of Si self-diffusion coefficients in SiO_2 from the experiments during oxidation and under oxidation-prevented condition by SiN capping layers (Ref. 12): □, ○, and △ represent the present results during oxidation with 1% oxygen at 1250, 1200, and 1150 °C, respectively. The dashed lines show the thermal equilibrium Si self-diffusivities from Ref. 14. Solid lines are the guides for the eyes.

structure, where the thick $^{28}SiO_2$ layer is prepared to avoid the effect of the SiO_2/Si interface and its value agrees well with the Si self-diffusivity in fused silica.[15] Moreover, we confirmed that the diffusivities also reach the thermal equilibrium values in the experiments at 1200 and 1250 °C. This enhanced diffusivity indicates that the emitted Si species from the SiO_2/Si interface enhances Si self-diffusivity near the SiO_2/Si interface; however, as the thickness of the grown $^{28}SiO_2$ layer increases, its influence to the ^{30}Si diffusivity in the $^{nat}SiO_2/^{28}SiO_2$ interface region reduces. Since a larger number of Si species are emitted under higher oxygen partial pressure,[16] it could be assumed that the faster oxidation causes the higher diffusivity enhanced by emitted Si species; however, Fig. 3 does not show a significant difference between the results in higher and lower oxygen fractions within the error range. One possible explanation is that the higher oxygen fraction causes more efficient oxidation of emitted Si species in the SiO_2 layer and, hence, decreases the number of Si species, which would have enhanced the Si self-diffusion.

In Fig. 4, our data on 1150, 1200, and 1250 °C oxidations are compared with the reference data on Si self-diffusivity in SiO_2. The enhanced diffusivity of the present study decreases to reach the thermal equilibrium value significantly faster than that in the oxidation-prevented ambient by SiN capping layers.[12] This result also indicates that the emitted Si species are absorbed into SiO_2 layer by oxidation before they reach the $^{nat}SiO_2/^{28}SiO_2$ interface in the oxidation ambient. Besides, Uematsu et al.[17] obtained the Si self-diffusivities via emitted Si, that is, the diffusivity exactly at the SiO_2/Si interface without the influence of oxygen, from the simulation in the same manner as in Ref. 18, which are 4.0×10^{-16}, 2.0×10^{-15}, and 6.0×10^{-15} cm^2/s at 1150, 1200, and 1250 °C, respectively. Therefore, it is obvious that the enhancement of Si self-diffusivity by the emitted Si during oxidation falls dramatically as the Si species are diffusing through SiO_2 and absorbed there.

In conclusion, we have succeeded in observing the enhanced Si self-diffusion near the SiO_2/Si interface during oxidation from the observation of ^{30}Si diffusion profiles in the $^{nat}SiO_2/^{28}SiO_2/^{28}Si$ structure. The Si self-diffusivity significantly decreases with increasing distance from the SiO_2/Si interface during oxidation compared with that under oxidation-prevented conditions. In addition, the Si self-diffusivity during oxidation approaches the thermal value as the $^{28}SiO_2$ thickness increases. These results indicate that Si species are emitted from the interface, enhance Si self-diffusion in SiO_2, and are quickly oxidized near the SiO_2/Si interface. The present study shows direct experimental evidence of the Si emission to SiO_2 during oxidation and provides the enhanced Si self-diffusivity in SiO_2 during thermal oxidation, which helps us to understand the fundamentals of the oxidation.

[1] B. E. Deal and A. S. Grove, J. Appl. Phys. **36**, 3770 (1965).
[2] H. Kageshima, K. Shiraishi, and M. Uematsu, Jpn. J. Appl. Phys., Part 2 **38**, L971 (1999).
[3] M. Uematsu, H. Kageshima, and K. Shirashi, Jpn. J. Appl. Phys., Part 2 **39**, L699 (2000).
[4] H. Kageshima and K. Shiraishi, Phys. Rev. Lett. **81**, 5936 (1998).
[5] A. M. Stoneham, C. R. M. Grovenor, and A. Cerezo, Philos. Mag. B **55**, 201 (1987).
[6] Y. Takakuwa, M. Nihei, and N. Miyamaoto, Appl. Surf. Sci. **117/118**, 141 (1997).
[7] D. Yu, G. S. Hwang, T. A. Kirichenko, and S. K. Banerjee, Phys. Rev. B **72**, 205204 (2005).
[8] Z. Ming, K. Nakajima, M. Suzuki, K. Kimura, M. Uematsu, K. Torii, S. Kamiyama, Y. Nara, and K. Yamada, Appl. Phys. Lett. **88**, 153516 (2006).
[9] S. M. Hu, Appl. Phys. Lett. **27**, 165 (1975).
[10] S. Hosoi, K. Nakajima, M. Suzuki, K. Kimura, Y. Shimizu, S. Fukatsu, K. M. Itoh, M. Uematsu, H. Kageshima, and K. Shiraishi, Nucl. Instrum. Methods Phys. Res. B **249**, 390 (2006).
[11] I. J. R. Baumvol, C. Krug, F. C. Stedile, F. Gorris, and W. H. Schulte, Phys. Rev. B **60**, 1492 (1999).
[12] S. Fukatsu, T. Takahashi, K. M. Itoh, M. Uematsu, A. Fujiwara, H. Kageshima, Y. Takahashi, K. Shiraishi, and U. Gösele, Appl. Phys. Lett. **83**, 3897 (2003).
[13] S. Hofmann, Surf. Interface Anal. **21**, 673 (1994).
[14] T. Takahashi, S. Fukatsu, K. M. Itoh, M. Uematsu, A. Fujiwra, H. Kageshima, Y. Takahashi, and K. Shiraishi, J. Appl. Phys. **93**, 3674 (2003).
[15] G. Brebec, R. Seguin, C. Sella, J. Bevenot, and J. C. Martin, Acta Metall. **28**, 327 (1980).
[16] M. Uematsu, H. Kageshima, and K. Shirashi, Jpn. J. Appl. Phys., Part 2 **39**, L952 (2000).
[17] M. Uematsu, K. Ibano, and K. M. Itoh (unpublished).
[18] M. Uematsu, M. Gunji, and K. M. Itoh, Defect Diffus. Forum **258–260**, 554 (2006).